

# *Update on the EUSO photodetector design*

**Alessandro Petrolini**

on behalf of the INFN - Genova

## General considerations

Focal surface (FS) geometry and macro-cells layout

Micro-cell design

⇒ Flavio's talk

Some critical items

Optical adapters for the R7600 MAPMTs

Information required from other sub-groups

The photo-detector simulation

⇒ Marco's talk

Work supported by ASI and INFN

- *Study report on the EUSO photo-detector design*, INFN note INFN/AE-01/04, 6 April 2001, available at: <http://wwwsis.lnf.infn.it/pub/INFN-AE-01-04.pdf>.
- *EUSO: the focal surface photo-detector*, ICRC 2001.
- Web Site: <http://www.ge.infn.it/euso>.

# General considerations (1)

## The photo-detector

- The photo-detector is one, single and complex instrument .  
It includes:
  - the sensors ;
  - the optical adapters (light collection system);
  - the front-end, trigger and data-handling electronics ;
  - the focal surface layout, structure and engineering, its integration with the support structure and ISS;
  - the interfaces between the different components;
  - all the ancillary systems required for the proper operation and control of the photo-detector.

It is arranged in micro-cells and macro-cells .

- All studies have been carried on assuming as boundary conditions:
  - no *R&D* allowed, only use available technology;
  - instrument ready in 2007 (?).
- If boundary conditions change, the solution to the equations will change.

## General considerations (2)

### The sensor

- We proposed to use commercial MAPMT for an *AirWatch*-like photo-detector in 1998 , as the most (or, probably, the only) viable option .
- MAPMT are a well established technology , available from shelf, with a solid basis and experience in industry and characteristics and a price which are easily quantified .
- The proposed model are on the market since a few years: their characteristics have been steadily improving over time thanks to the manufacturer's experience and user's feedback
- The proposed models have been (and will be) used in space applications.
- Other alternatives are appealing, but they are not ready for use in the short term.

# Focal surface geometry basics

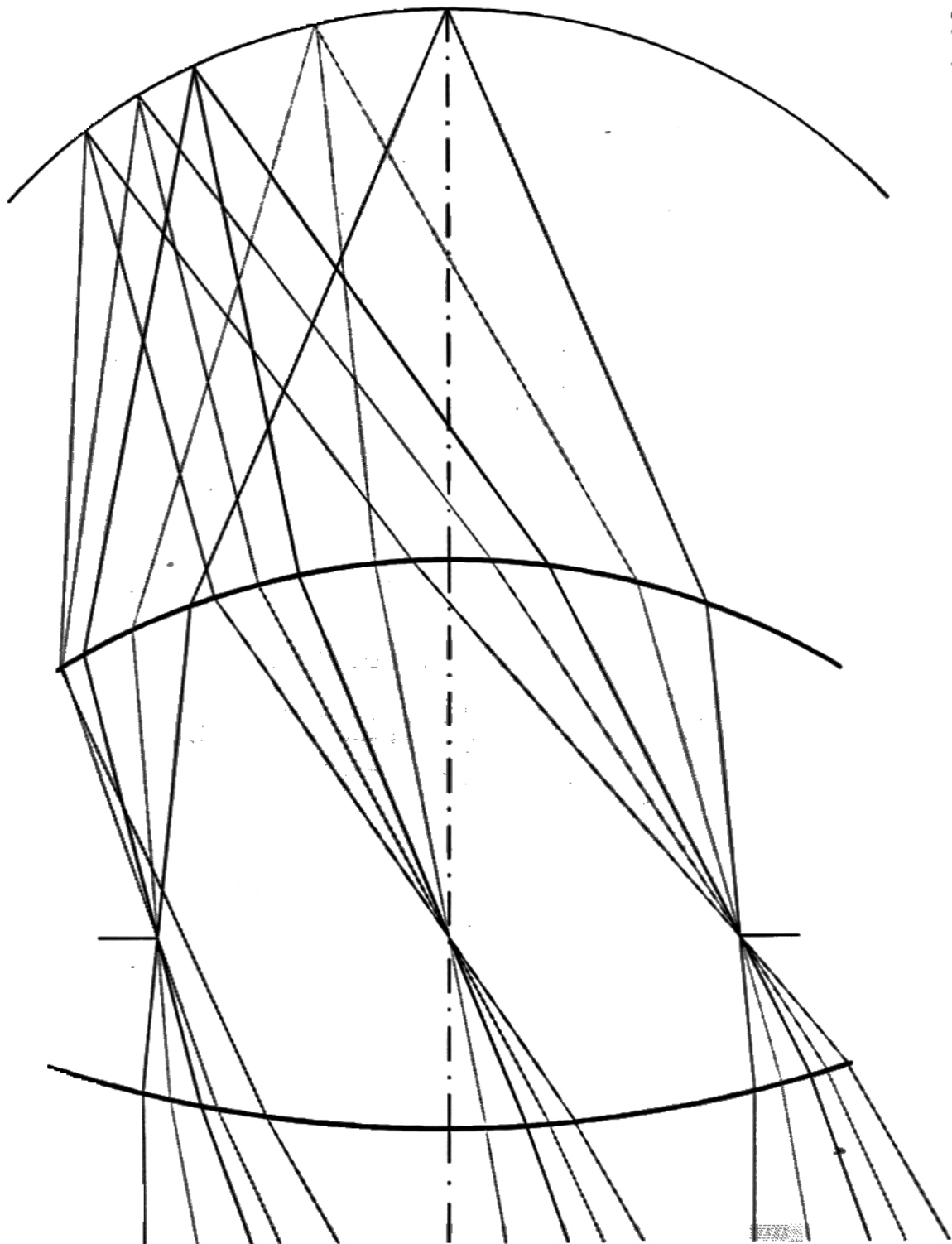
## The focal surface from the optics design

- Assume the (provisional) optics design from the IDD:  
 $LD = 2.5$  m;  $EPD = 2.0$  m;  $f/\# = 1.25$ ;  $FoV = \pm 30^\circ$  .
- Provisional geometry of the focal surface  
(from the provisional design of the main optics): **paraboloid**  
( $z \sim \alpha r^2$ ;  $\alpha = 0.312 \text{ m}^{-1}$ ; maximum  $r \simeq 1.15$  m).
- Radius of curvature (**highly non-spherical**):  
 $\rho \simeq 1.6$  m at the vertex;  $\rho \simeq 3.0$  m at the edge of FoV.
- More detailed and **more** precise **information is needed** .

## General considerations

Fill the focal surface as much as possible with MAPMTs.

- Basic unit: MAPMT (flat input window and square section).  
The physical size is the same for M16 and M64.  
Assumed **MAPMT pitch: 27.0 mm** .
- The focal surface can (*must?*) be fitted with **flat modules**  
with a suitable dimension and shape.  
*A priori* a photodetector module is different from a macro-cell.
- A non-flat focal surface cannot be tessellated exactly  
(i.e. without *holes*) by means of rectangular shapes:  
**some loss** in the geometrical acceptance,  
due to the focal surface tessellation, **cannot be avoided** .
- This geometrical acceptance loss mainly affects the number  
of detected EAS, not the single photon detection efficiency.



500 00 MM

Monochromatic Double Fresnel,  $f/1.25$  Scale: 0.05 DJL 20-Feb-01

## FS geometry basics: external inputs

- For a given local radius of curvature of the focal surface,  $R$ , and rectangular module of sides  $a$  and  $b$ , with  $L = \sqrt{a^2 + b^2}$ , the maximum discrepancy is given by the relation:

$$\Delta z \simeq 0.5 \cdot R \left[ 1 - \sqrt{1 - L^2/(4R^2)} \right] \simeq 0.5 \cdot L^2/(8R) \quad \text{if } L \ll R$$

$$a = b = 172 \text{ mm} \quad \implies \quad \Delta z \simeq 1.2 \text{ mm} \div 2.3 \text{ mm}$$

$$a = b = 226 \text{ mm} \quad \implies \quad \Delta z \simeq 2.1 \text{ mm} \div 4.0 \text{ mm}$$

- Approximate defocusing in the direction tangential to the FS,  $\Delta w$ , produced by a small displacement  $\Delta z$  in the direction perpendicular to the focal surface:

$$\Delta w \approx \Delta z \tan \theta_{max} \simeq \Delta z/(2f\#)$$

$$\left( \implies \Delta w \simeq 0.9 \text{ mm} \div 1.6 \text{ mm} \right).$$

- Module size: ensure that a good fraction of EAS is (almost) fully contained inside a single module.
- **Simplify** the design: use only one/two different modules.
- Take into account the unavoidable **dead region at the edge** of each module, required for the mechanical support.
- The approximate probability that any EAS starting inside a rectangular module of sides  $a$  and  $b$  is fully contained in the module, is given by:

$$\text{Prob} \approx 1 - \frac{(a+b)l}{ab} + \frac{9l^2}{4ab} \quad l < a/2, l < b/2$$

$$a = b = 2l \quad \implies \quad \text{Prob} \simeq 0.56$$

# Focal surface layout(s)

## Some possible layouts

- Simplifying assumption: the vertex of modules lay on the FS. In the final design the maximum distance of module to the focal surface will be minimized.
- the module sizes  $6 \times 6$ ,  $6 \times 8$  and  $8 \times 8$  seem to be the most promising, due to the constraints;
- layout with **maximum filling** and **some symmetry** (preferred).

## General conclusions

- The next step requires more detailed and precise input data.
- Different layouts lead to **similar overall results** (i.e. filling factors)  $\implies$  use any layout with confidence.
- **The angular granularity is fixed by the MAPMT characteristics** (taking into account a suitable optical adapter):
  - M16:  $\Delta\alpha \simeq 0.16^\circ$   
 $\implies \Delta x_E \simeq 1.0 \div 1.2$  km ( $0.97 \cdot 10^5$  channels)
  - M64:  $\Delta\alpha \simeq 0.08^\circ$   
 $\implies \Delta x_E \simeq 0.5 \div 0.6$  km ( $3.87 \cdot 10^5$  channels)
- Different pixel sizes can be used to match the optics Point Spread Function (PSF).
- Example: six-fold symmetric  $6 \times 6$  MAPMTs layout
  - number of modules = 168; number of MAPMTs = 6048.
  - Maximum discrepancy form the ideal surface for a  $6 \times 6$  module:  $\lesssim 1.5$  mm.

# FS layout: Maximum filling - B6-6 × 6

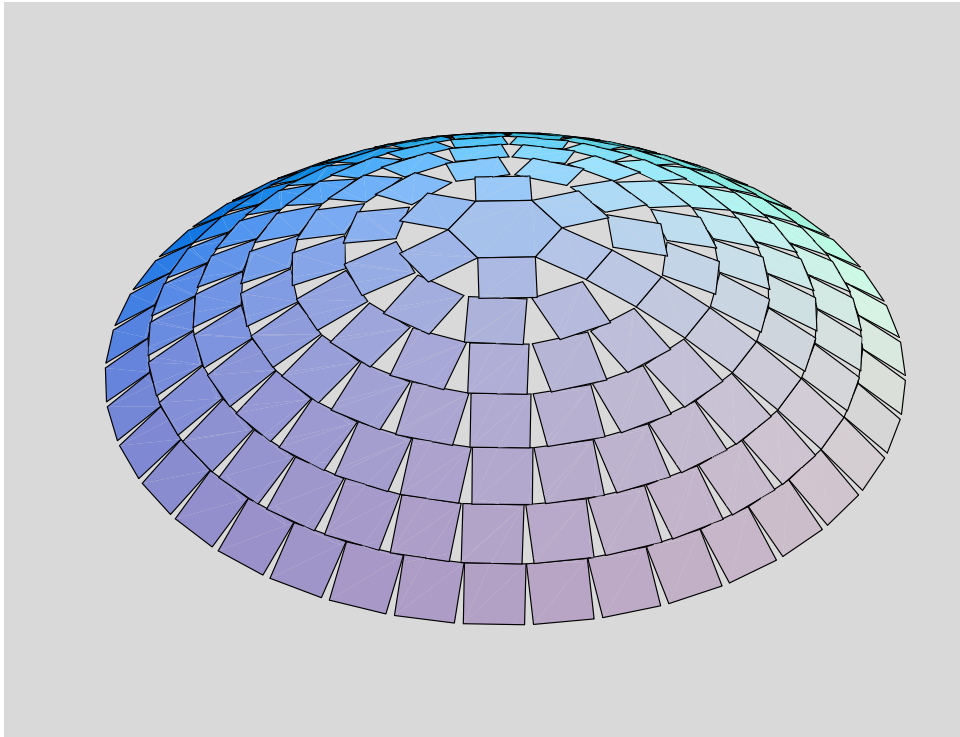


Figure 1: FS layout

```
=====
Rectangle sizes (mm) {tangential/radial} : { +172.000, 172.000}
Ideal progression with n-fold symmetry : {6,12,18,24,30,36,42}
Number of modules in row is : {6,11,17,23,29,34,40}
Total number of modules : 160
Starting from angle : 3.4108
Ending at angle : 27.1812
Required ending angle : 24.8127
Filling factor : 0.858433
Approx Filling factor central polyogn : 0.0139392
Paraboloid's area up to coverage (m^2) : 5.51405
Angular range starts at (deg){+3.411, +6.584, +9.916, +13.297, +16.712, +20.161, +23.649}
Angular range ends at (deg) {+6.584, +9.916, +13.297, +16.712, +20.161, +23.649, +27.181}
DELTA Angular range (rad) {+0.055, +0.058, +0.059, +0.060, +0.060, +0.061, +0.062}
Max discrepancy (mm) {+4.510, +4.329, +4.091, +3.825, +3.555, +3.297, +3.059}
Max estimated defocusing (mm){+1.804, +1.732, +1.636, +1.530, +1.422, +1.319, +1.224}
Max discrepancy at theta {+4.645, +8.041, +11.445, +14.864, +18.307, +21.781, +25.295}
Max discrepancy central polygon (mm) : +9.261
Gap :{+172.381,+109.098, +69.165, +48.771, +35.614, +31.757, 22.961}
=====
```



# FS layout: Maximum filling - B8-6 × 6

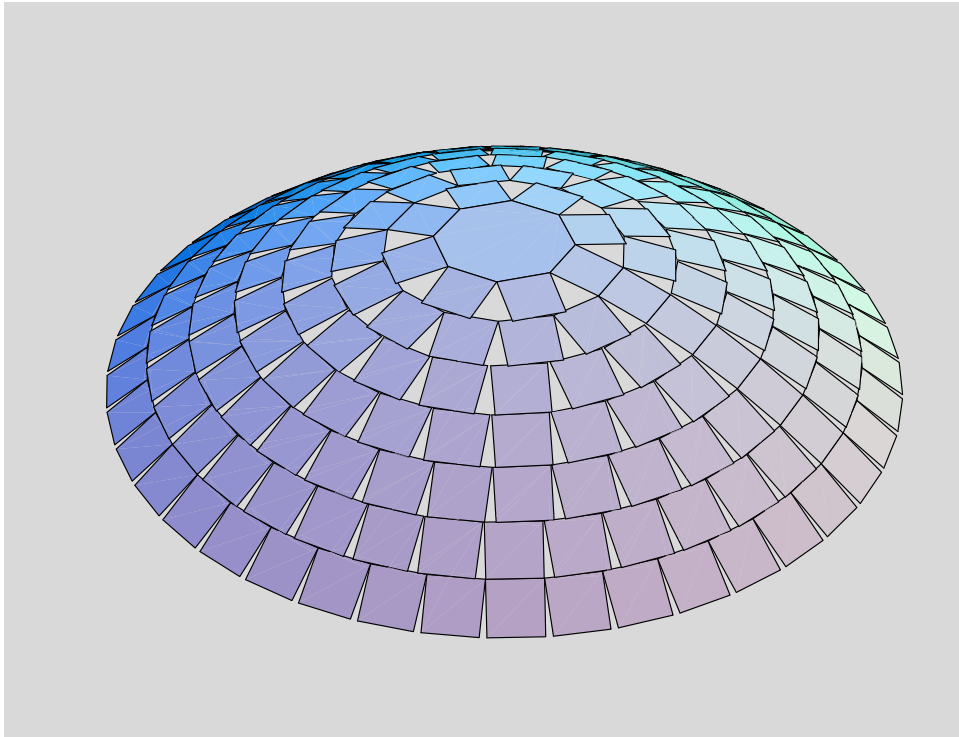


Figure 2: FS layout

```

=====
Rectangle sizes (mm) {tangential/radial} : { +172.000, +172.000}
Ideal progression with n-fold symmetry : {8,16,24,32,40,48,56}
Number of modules in row is : {8,14,19,25,31,36,42}
Total number of modules : 175
Starting from angle : 4.46099
Ending at angle : 28.4044
Required ending angle : 24.8127
Filling factor : 0.865405
Approx Filling factor central polyogn : 0.0238774
Paraboloid's area up to coverage (m^2) : 5.9824
Angular range starts at (deg){+4.461, +7.719, +11.072, +14.465, +17.891, +21.353, +24.855}
Angular range ends at (deg) {+7.719, +11.072, +14.465, +17.891, +21.353, +24.855, +28.404}
DELTA Angular range (rad) {+0.057, +0.059, +0.059, +0.060, +0.060, +0.061, +0.062}
Max discrepancy (mm) {+4.456, +4.252, +4.001, +3.732, +3.465, +3.213, +2.983}
Max estimated defocusing (mm){+1.783, +1.701, +1.601, +1.493, +1.386, +1.285, +1.193}
Max discrepancy at theta {+5.809, +9.207, +12.616, +16.042, +19.495, +22.982, +26.511}
Max discrepancy central polygon (mm) : +15.797
Gap :{+130.289, +73.711, +61.634, +44.214, +32.388, +28.846, +20.598}
=====

```

# FS layout: Symmetric - B6-6 × 6

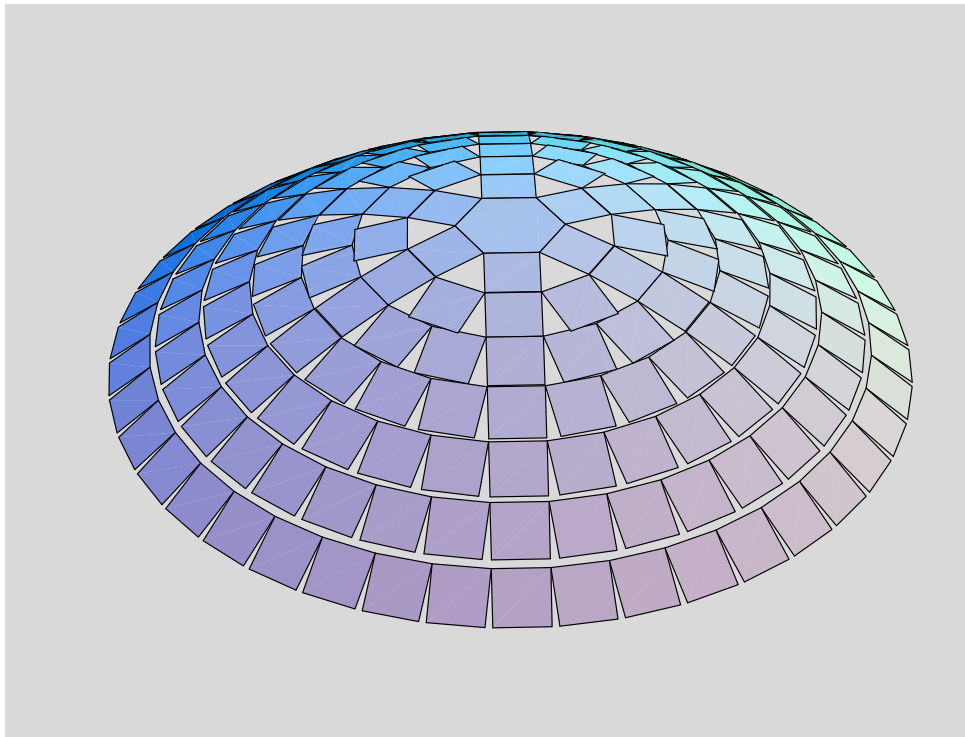


Figure 3: FS layout

```
=====
Rectangle sizes (mm) {tangential/radial} : { +172.000, 172.000}
Ideal progression with n-fold symmetry : {6,12,18,24,30,36,42}
Number of modules in row is : {6,12,18,24,30,36,42}
Total number of modules : 168
Starting from angle : 3.4108
Ending at angle : 28.3878
Required ending angle : 24.8127
Filling factor : 0.831687
Approx Filling factor central polyogn : 0.0128618
Paraboloid's area up to coverage (m^2) : 5.97594
Angular range starts at (deg){+3.411, +6.620, +9.955, +13.411, +17.019, +20.816, +24.839}
Angular range ends at (deg) {+6.584, +9.953, +13.336, +16.827, +20.471, +24.312, +28.388}
DELTA Angular range (rad) {+0.055, +0.058, +0.059, +0.060, +0.060, +0.061, +0.062}
Max discrepancy (mm) {+4.510, +4.327, +4.088, +3.816, +3.531, +3.251, +2.984}
Max estimated defocusing (mm){+1.804, +1.731, +1.635, +1.526, +1.413, +1.300, +1.194}
Max discrepancy at theta {+4.645, +8.078, +11.484, +14.979, +18.617, +22.442, +26.495}
Max discrepancy central polygon (mm) : +9.261
Gap : {+172.381, 86.540, +56.377, +40.899, +31.446, +25.075, +20.505}
=====
```

# FS layout: Symmetric - B6-8 × 8

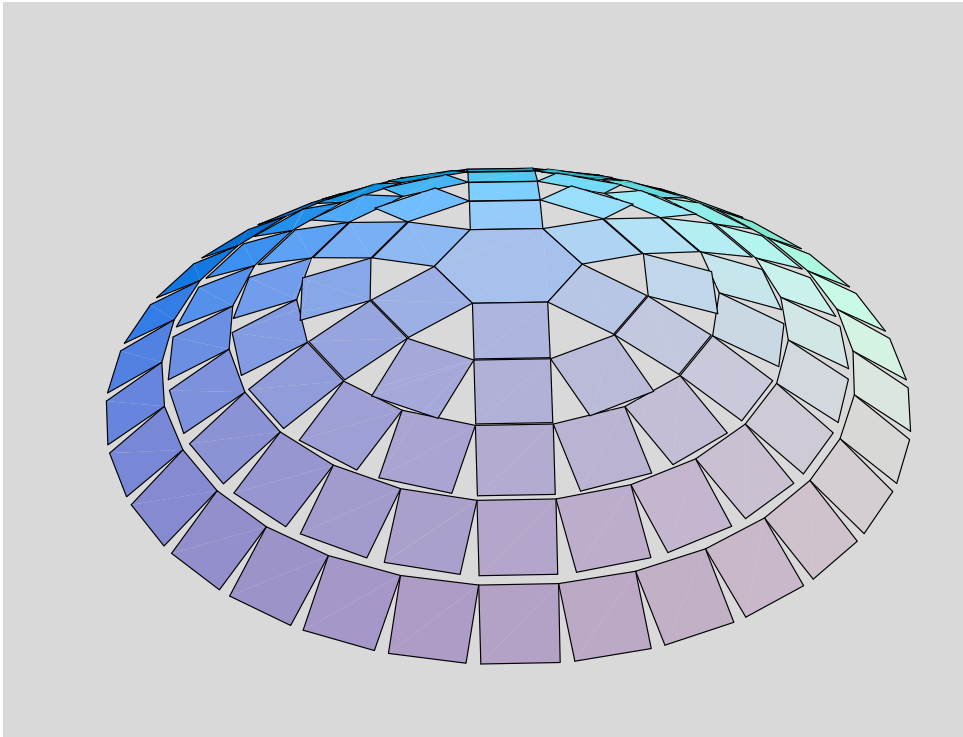
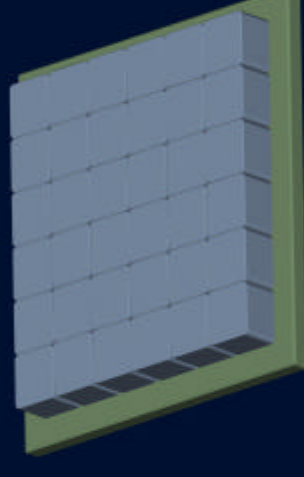
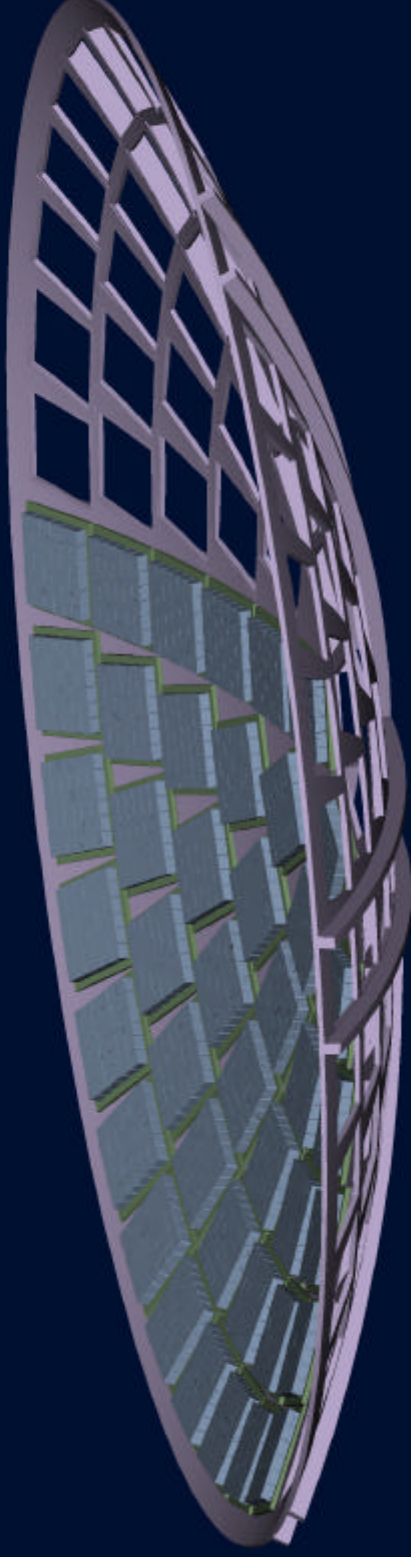


Figure 4: FS layout

```
=====
Rectangle sizes (mm) {tangential/radial} : { +226.000, +226.000}
Ideal progression with n-fold symmetry : {6,12,18,24,30}
Number of modules in row is : {6,12,18,24,30}
Total number of modules : 90
Starting from angle : 4.48636
Ending at angle : 27.7336
Required ending angle : 24.8127
Filling factor : 0.803122
Approx Filling factor central polyogn : 0.0231841
Paraboloid's area up to coverage (m^2) : 5.72372
Angular range starts at (deg){+4.486, +8.744, +13.236, +17.995, +23.098}
Angular range ends at (deg) {+8.661, +13.136, +17.710, +22.542, +27.734}
DELTA Angular range (rad) {+0.073, +0.077, +0.078, +0.079, +0.081}
Max discrepancy (mm) {+7.663, +7.156, +6.542, +5.898, +5.280}
Max estimated defocusing (mm){+3.065, +2.863, +2.617, +2.359, +2.112}
Max discrepancy at theta {+6.098, +10.645, +15.233, +20.051, +25.210}
Max discrepancy central polygon (mm) : +15.976
Gap :{+224.619,+111.275, +71.255, +50.708, +38.225}
=====
```

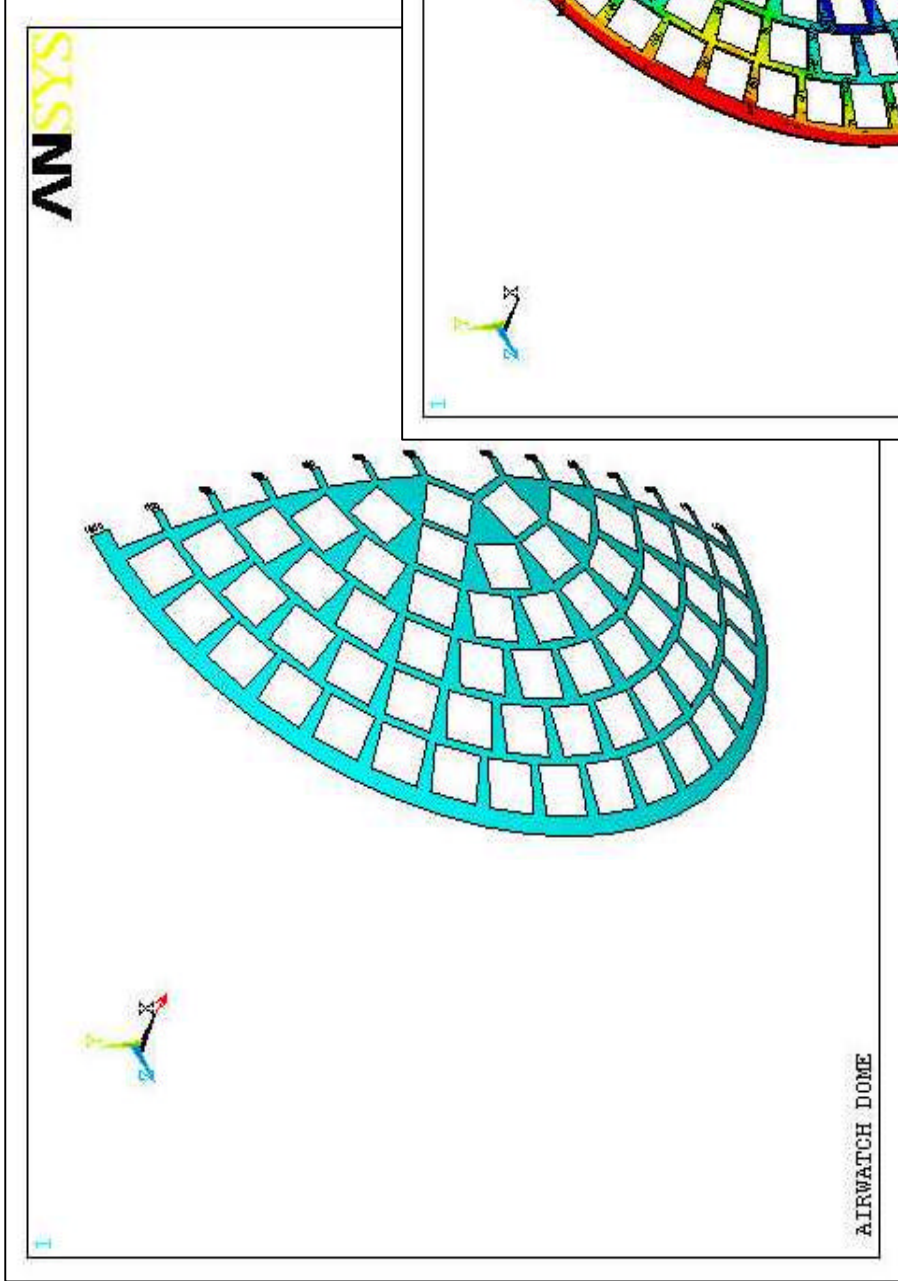
# MAPMTs support proposal

- Spherical focal surface curvature radius: 2500 mm
- Focal surface diameter: 2500 mm
- 4536 MAPMTs (126 modules)
- geometrical coverage: to be optimized
- Structure weight: about 25 Kg
- MAPMTs + lenses + base-board: about 300 kg
- Material: composite sandwich (two “12 unidirectional carbon pre-preg plies 0.3 mm thick” enclosing an aluminium honeycomb core 1/8” 15 mm thick)

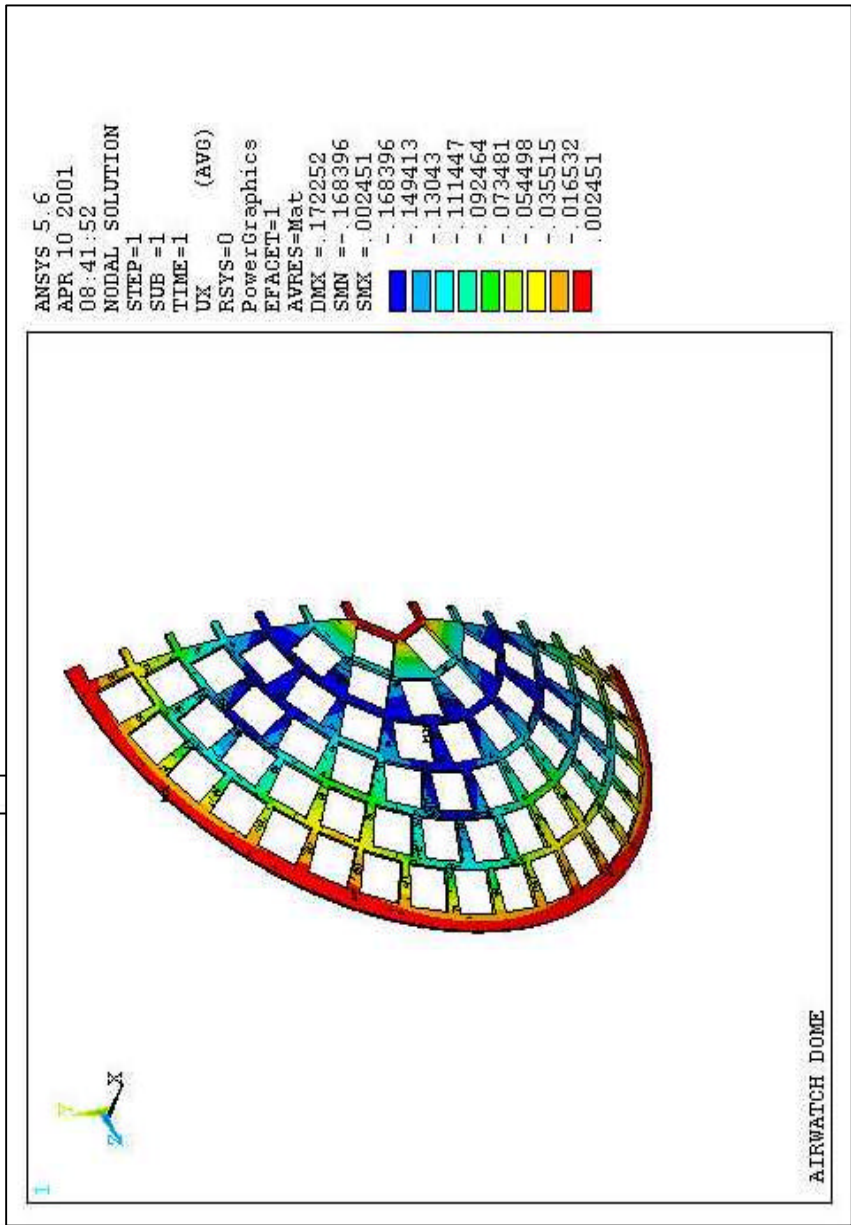


- 6x6 MAPMTs modules
- Base dimensions: 180x180 mm<sup>2</sup> (to be optimized)
- MAPMTs array dimensions: 162x162 mm<sup>2</sup>
- Clearance between MAPMTs: 1.3 mm
- Lenses glued on the MAPMT window

# MAPMT support FEA analysis

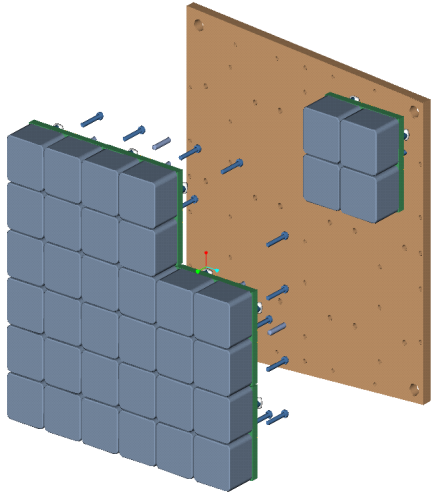
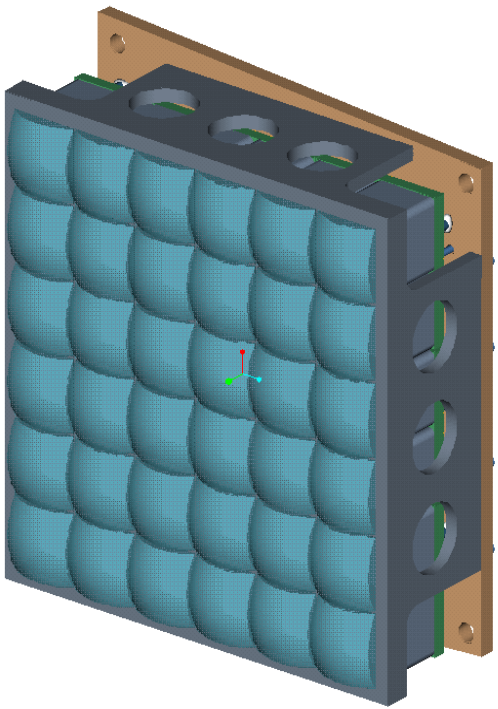
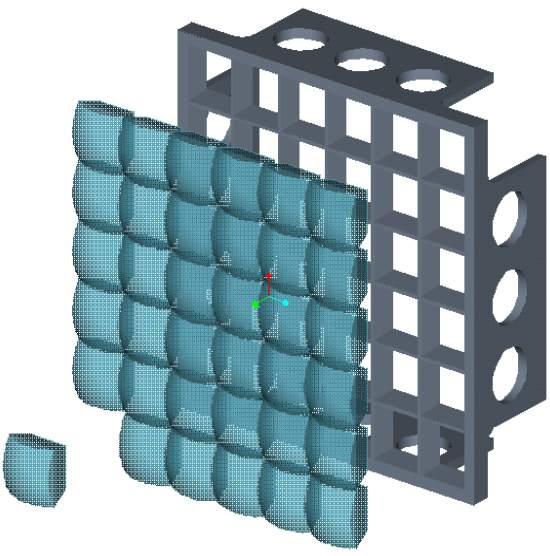


- **LOAD: 1 g ALONG POSITIVE X AXIS**
- **MASS: 320 Kg, UNIFORM**
- **CONSTRAINTS: UX=UY=UZ=0 ON THE EXTERNAL EDGE, UX=0 ON THE INTERNAL EDGE**
- **REINFORCING RIBS ON THE BOTTOM NOT YET MODELED**

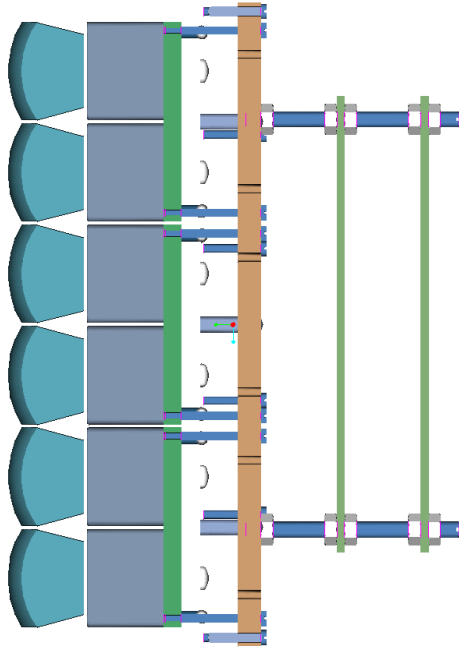
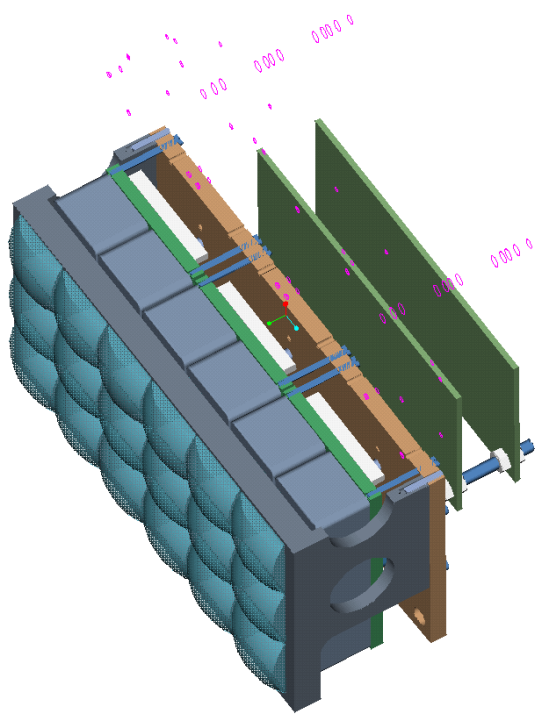
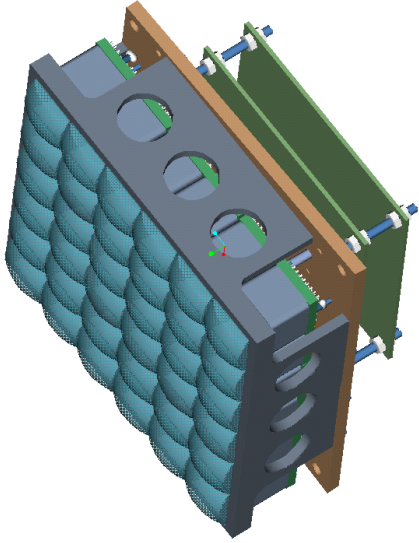


- **MAXIMUM DISPLACEMENT ALONG X: 0.17 mm**
- **FIRST MODAL FREQUENCY: 764 Hz**

# EUSO-FS: macro-cell/module design



# EUSO-FS: macro-cell/module design

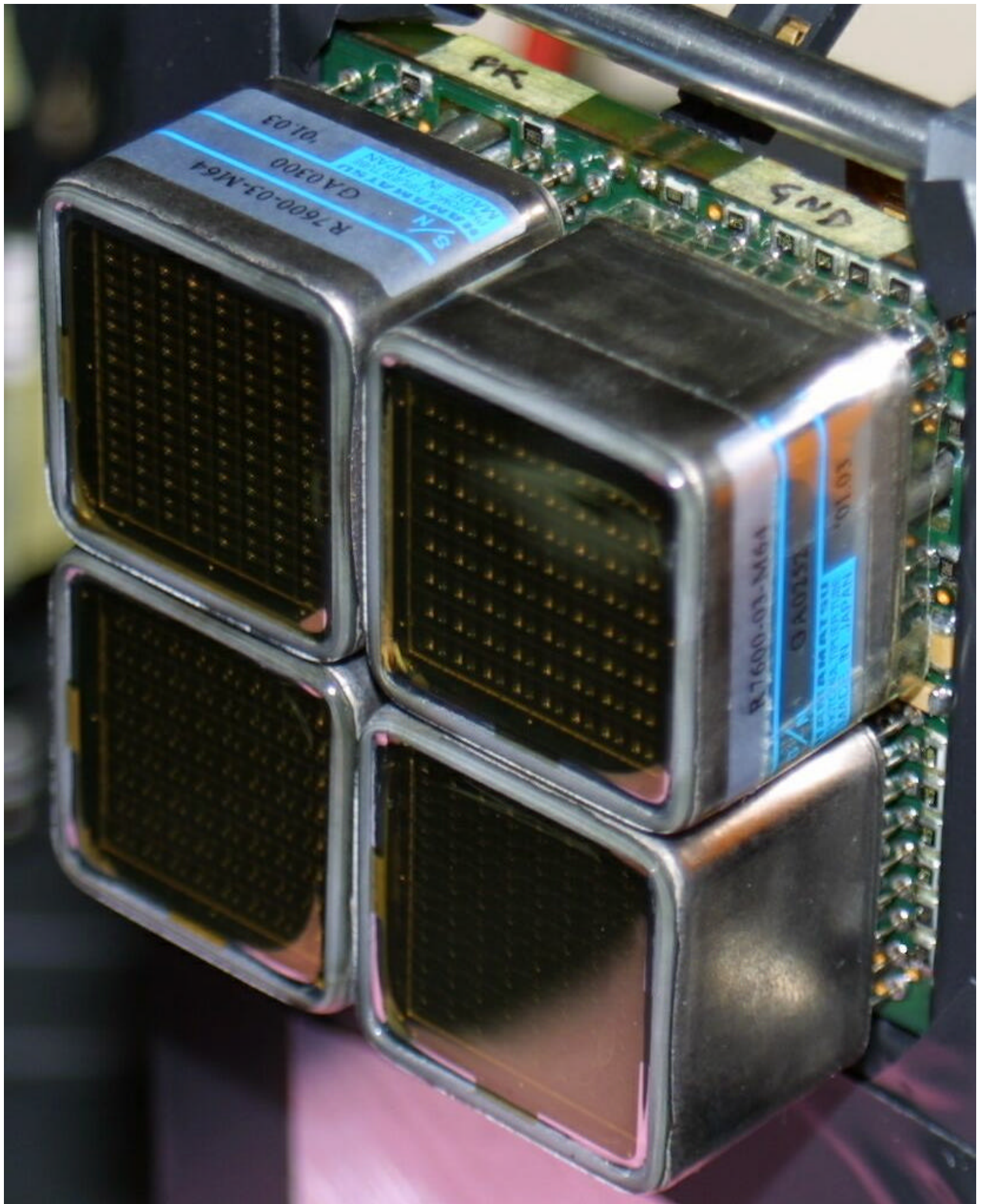


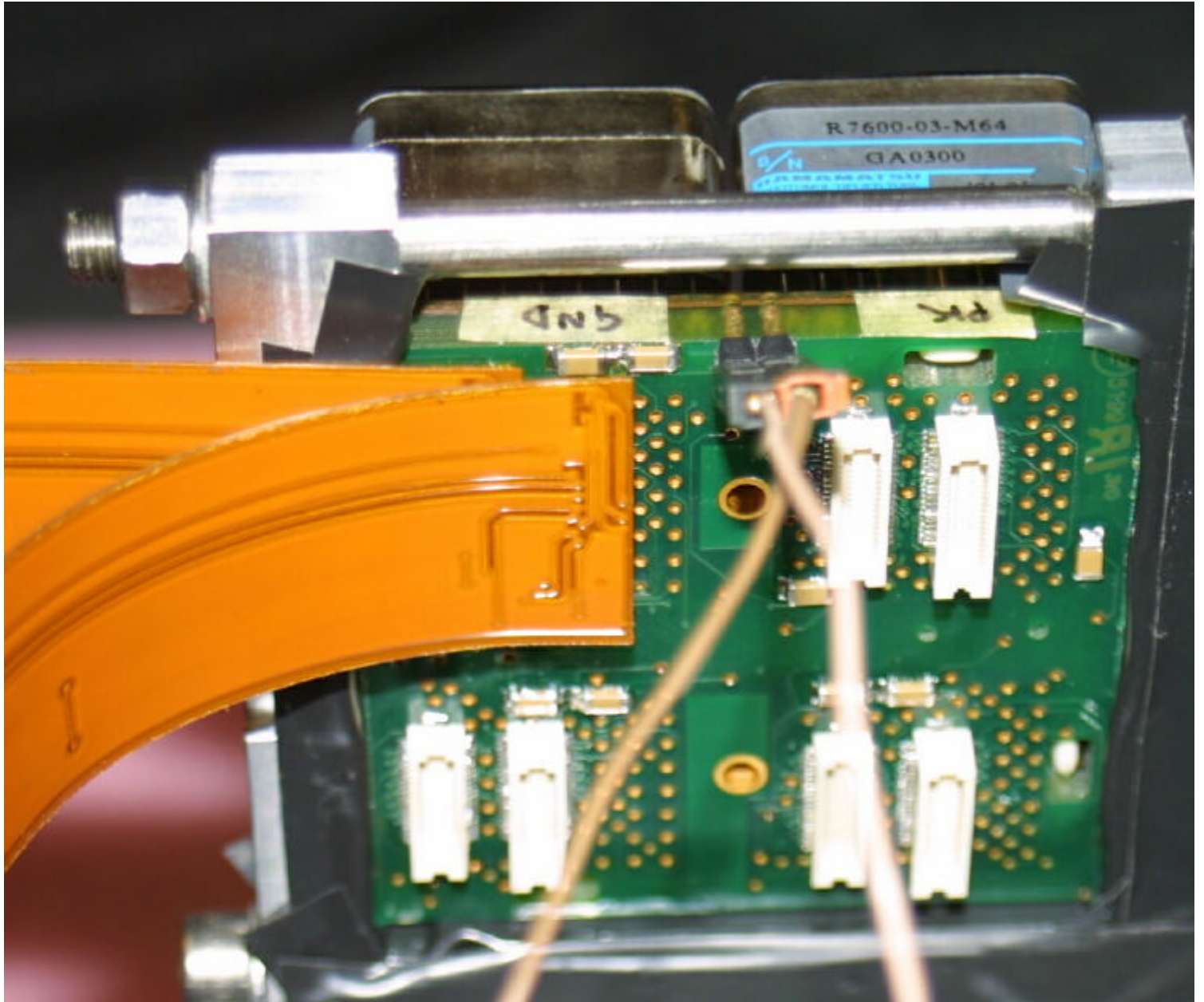
# The MAPMT base-board (micro-cell)

## Design

- Designed for  $2 \times 2$  MAPMTs: elementary unit ;  
one HV connection at the center; 1 ÷ 4 (?) voltage dividers.
- MAPMTs on one side and f/e electronics on the back-side :  
close to the detector, compact structure, minimize cabling.
- It accomplishes Close-packing of the MAPMTs  
as well as and close packing of base-boards  
(27 mm pitch in the base design).
- Thick PCB: self-supporting;  
a copper layer takes care of heat dissipation.
- Prototypes are available for the interested groups.







# Critical items

- MAPMT: Voltage divider optimization and power consumption minimization.
- MAPMT ageing:  
operate the MAPMT at low gain to reduce ageing as the real amount of light the MAPMT will receive on orbit is, to some extent, uncertain.  
Moreover the possibility to increase the HV during the mission to recover a possible gain decrease, must exist.
- HV/LV design.  
Evaluate the need for buffering batteries:
  - ISS does not guarantee power availability at any time, only average values.
  - Increase the effective power available to the electronics by exploiting the short observation duty cycle ?  
Is it compatible with the thermal control of the FS?
- Evaluate the environmental susceptibility.
- Overall mass reduction.

# Optical adapters for the MAPMTs

## General issues

- The geometrical acceptance of the bare MAPMT is  $\approx 0.45$ ; it becomes  $\approx 0.41$  including a realistic pitch between MAPMTs.
- The worst feature is not the overall low geometrical acceptance but the fact that it is not uniform on the surface :  
 $\implies$  discontinuous recording of the EAS.
- Some preliminary results are available (to be optimized); the results, normally, strongly depend on the photon incidence angle distribution .
- The impact on the photo-detector has to be evaluated (i.e. Cherenkov light produced by charged cosmic rays).
- All studies have been carried on with the M64 MAPMT; the M16 performances would be, normally, better.

## Work plan

- Some more optimization is required.
- The Firenze group will carry on additional studies.

## One option requiring some *R&D*

- Commercial fiber optic tapers, usually,
  - are not designed to work in the UV;
  - and have a low ( $\approx 0.75$ ) filling factor (sensitive to total area ratio) at the entrance face.

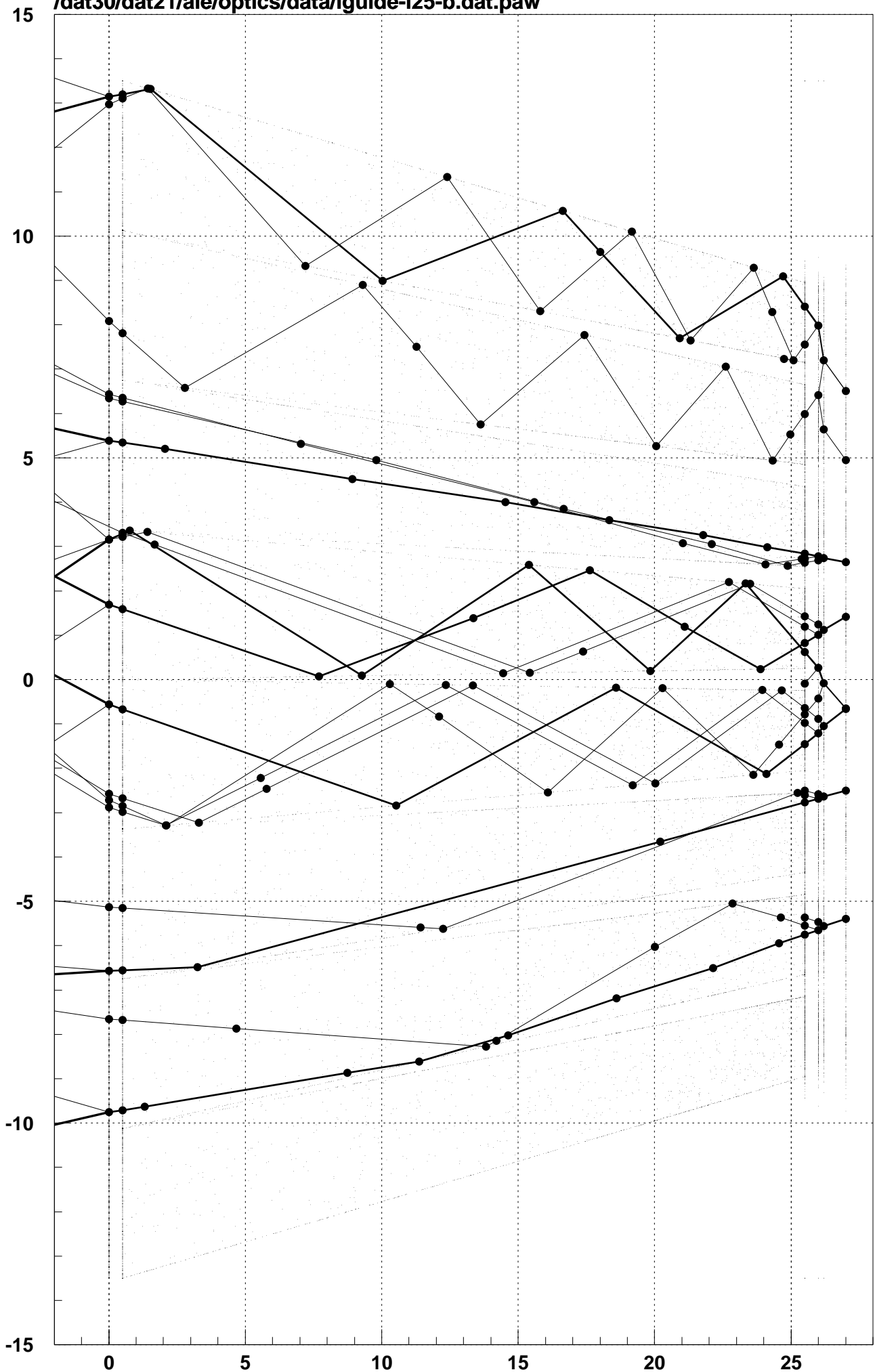
# Tapered Light pipes

## Tapered Light pipes

- Use a bundle of  $8 \times 8$  tapered light pipes, working by total internal reflection or by normal reflection. This creates an exact one-to-one correspondence between the (ideal) focal surface pixels and the (real) MAPMT pixels:
  - it avoids the inefficient region between pixels;
  - no image distortion is introduced.
- **Total internal reflection light pipes** require a highly transmissive and light-weight material (just like the main optics).
- **Reflecting light pipes** require a high reflectivity coating over a large range of incidence angles (up to grazing incidence) in the 300 nm ÷ 400 nm wavelength range.
- **The engineering of the device is not trivial** in both cases. See K. Arisaka's prototype.
- Work plan:
  - optimize the design, given the incident light distribution;
  - find the best material;
  - produce a realistic engineering of the design;
  - get a better estimate of cost;
  - evaluate the impact on the photo-detector.

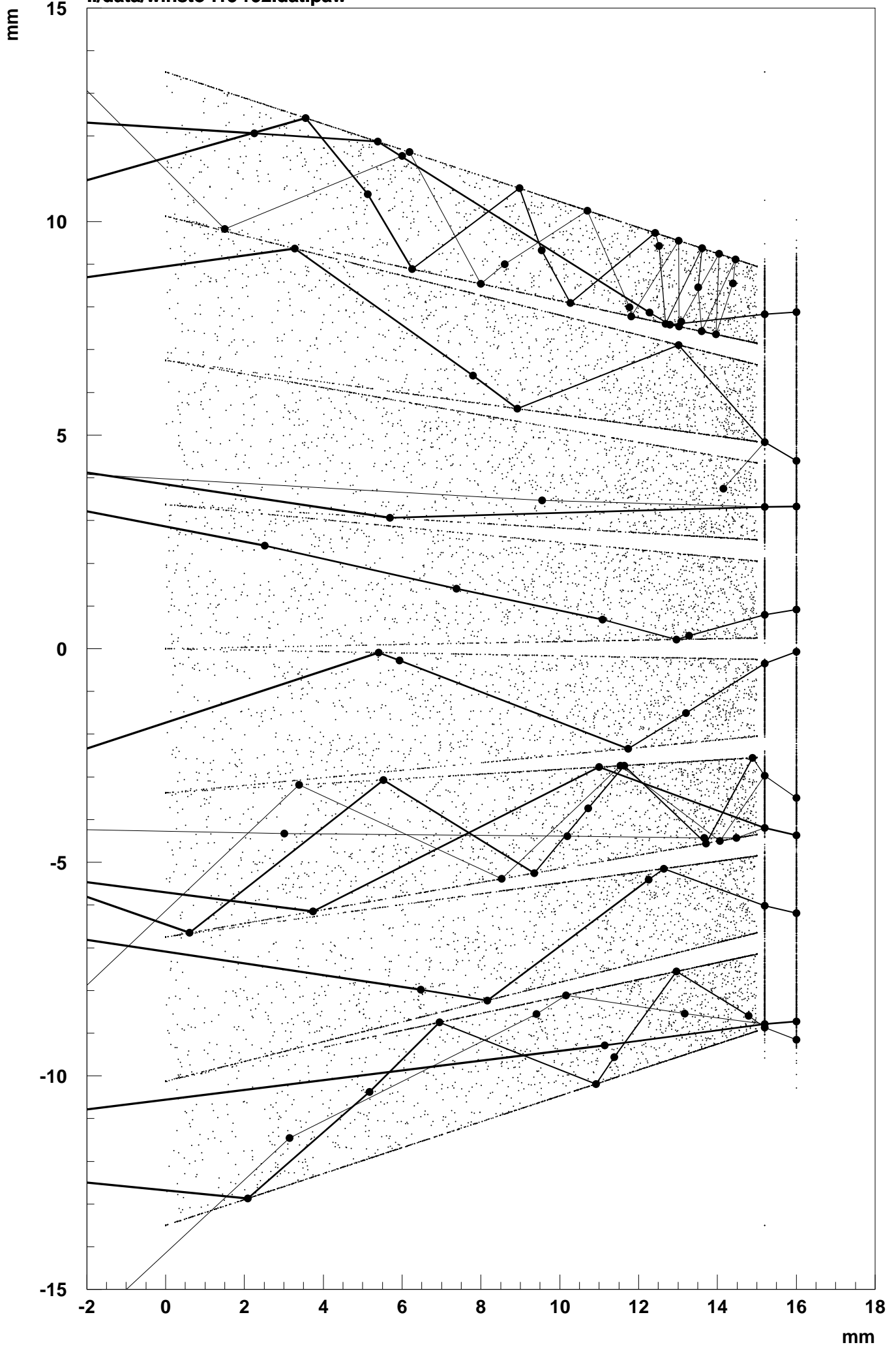
# Total internal reflection light pipes

/dat30/dat21/ale/optics/data/lguide-l25-b.dat.paw



# Reflecting light pipes: ray tracing

../data/winsto-l15-r92.dat.paw



# Optical adapters simulations

## Hypoteses

Try to assume as realistic as possible hypoteses.

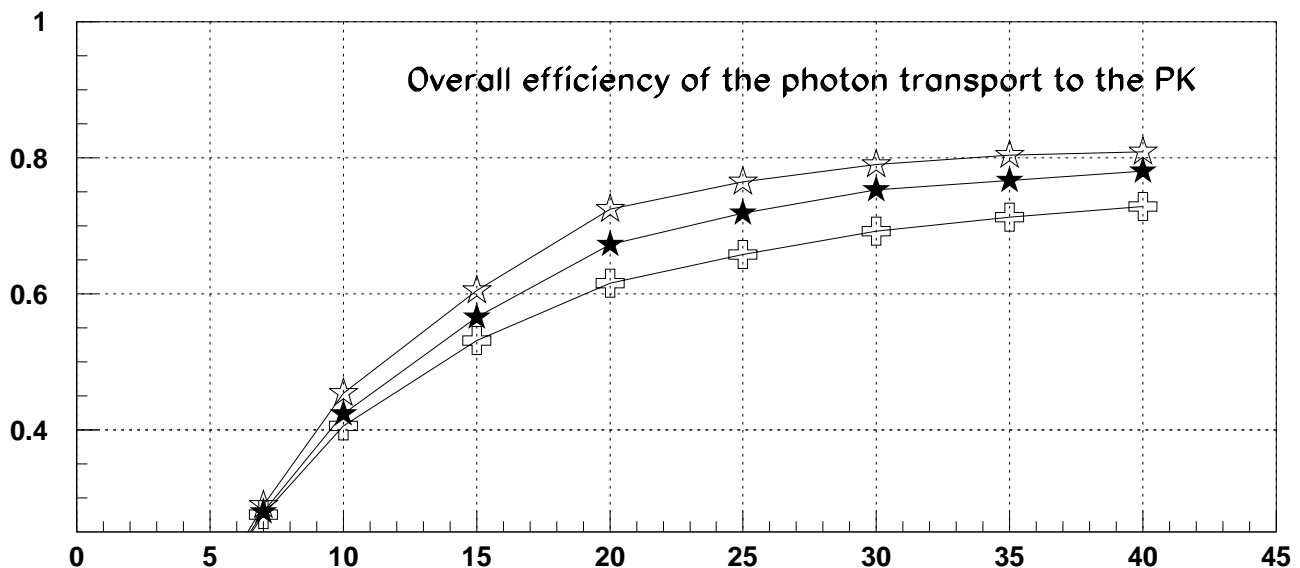
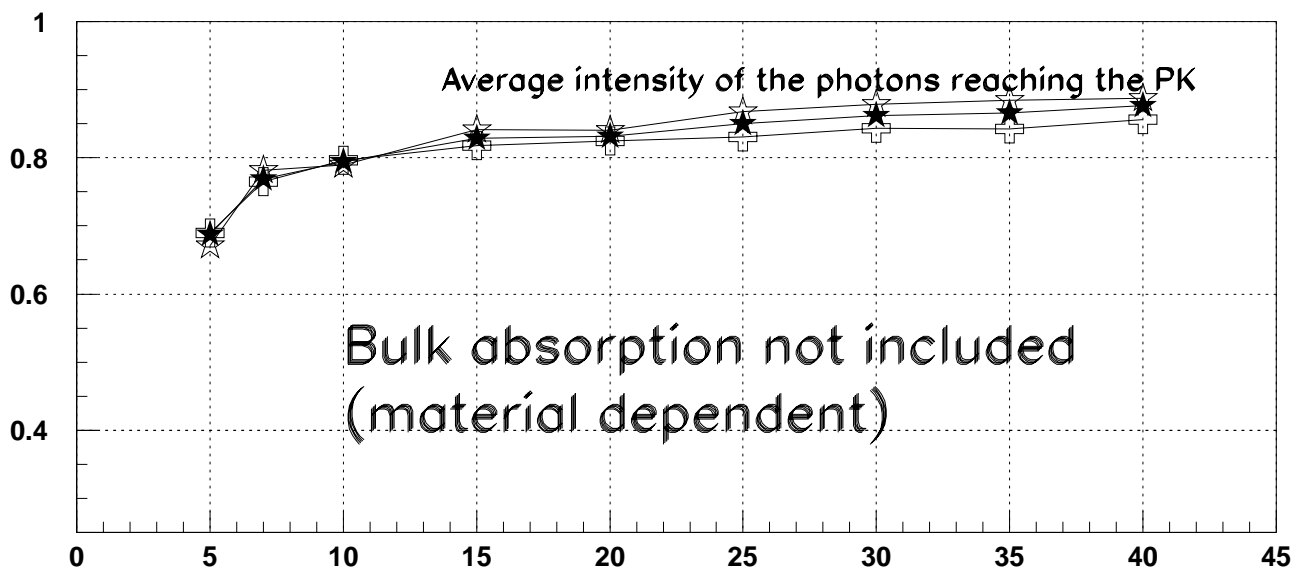
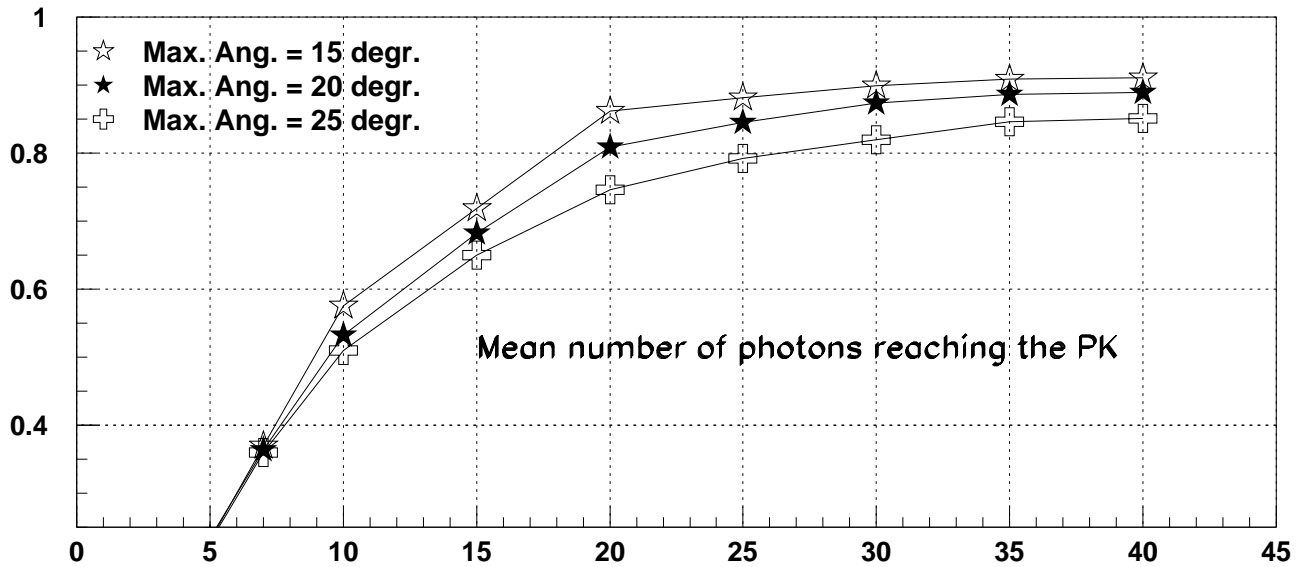
- MAPMT pitch: 27 mm (as in the baseline base-board).
- Inter-pixel inefficiency is accounted for.
- Fresnel refelction losses are accounted for.
- The MAPMT input window and a realistic mechanics are accounted for.
- All possible photon losses we could imagine (?) are accounted for.
- Note that photons might be lost with light pipes because they might bounce back !
- No inclusion of material-dependent properties: reflectivity and bulk absorption.  
Results are reported as a function of the material-dependent properties:  
properties can be calculated given the matierial properties.

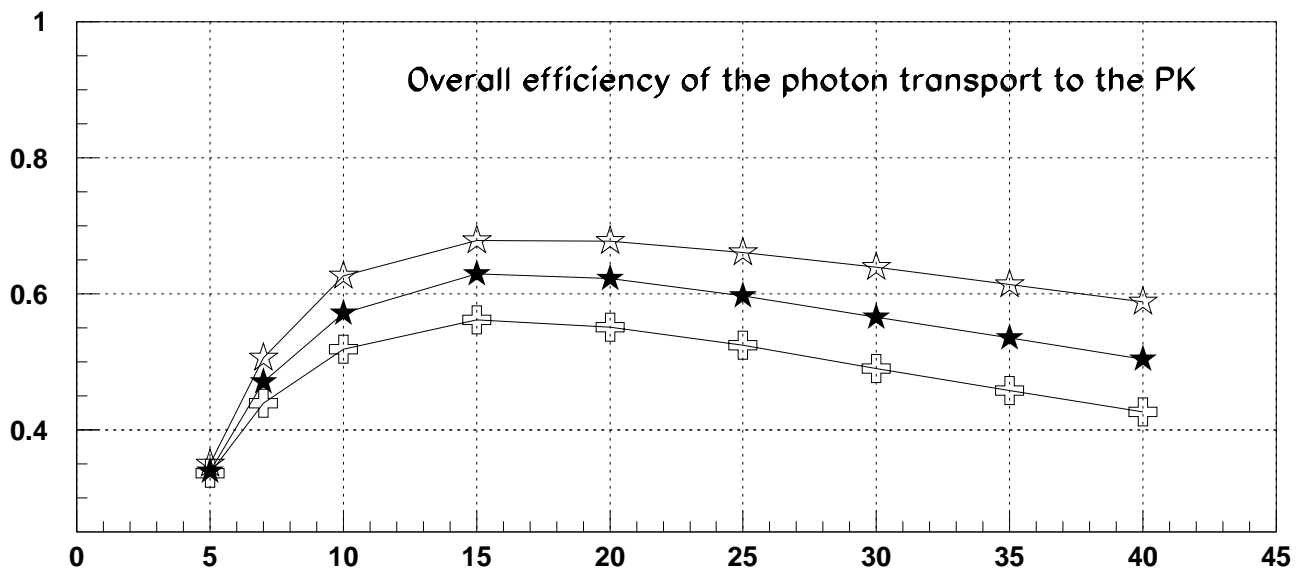
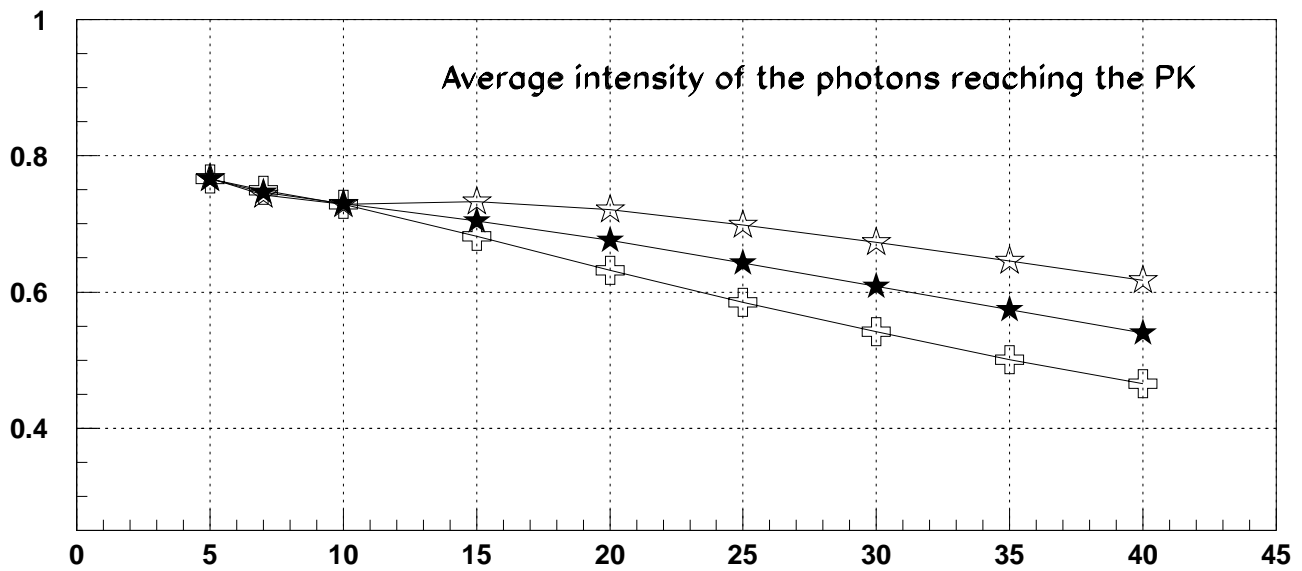
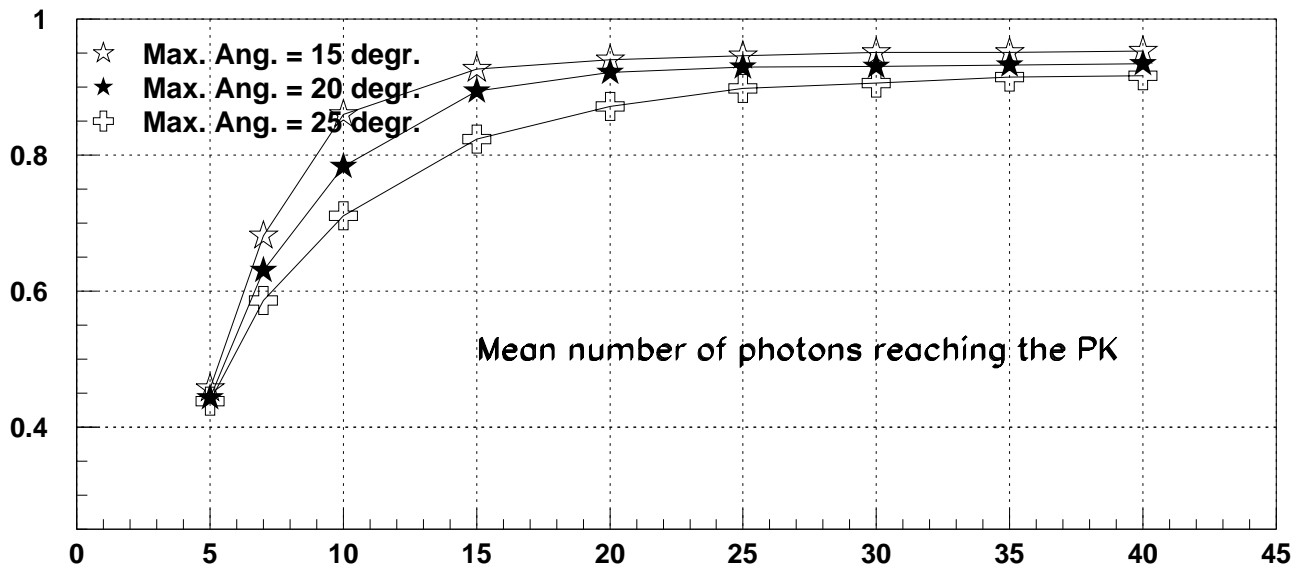
## Input rays

- Rays uniformly distributed on the FS.
- Uniform distribution of rays in solid angle up to a maximum incidence angle  $\theta_{max} = 25^\circ$ , close to the one of the EUSO optics.



# Total internal reflection light pipes

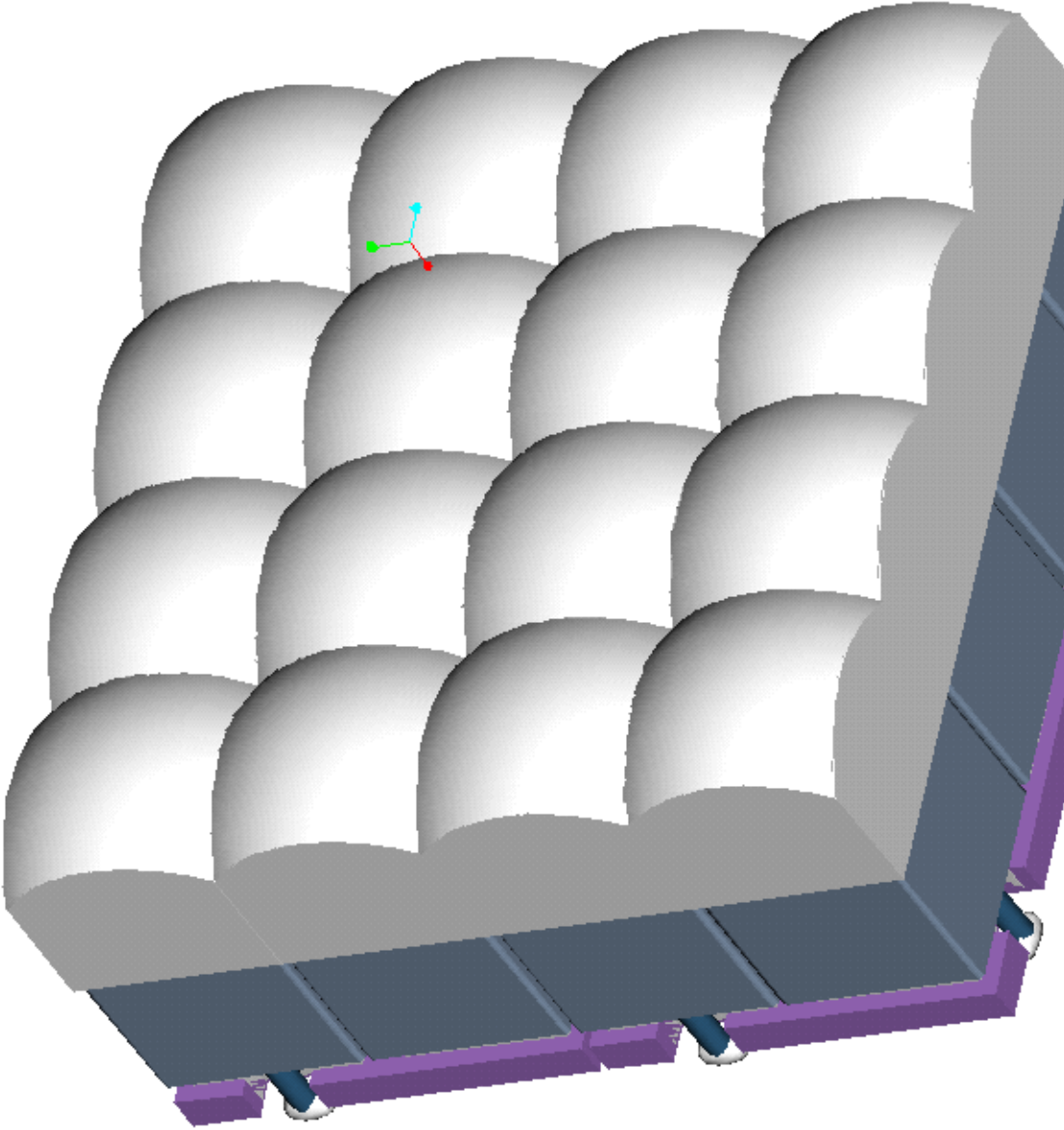




# Hemispherical lenses

## Hemispherical lenses

- A hemispherical lens in front of the MAPMT can provide the required demagnification and create an approximate one-to-one correspondence between the focal surface pixels and the (smaller) MAPMT pixels.
  - overall geometrical acceptance can increase to  $\approx 0.7$ ;
  - inefficient regions between pixels cannot be recovered;
  - the fraction of photons exactly reconstructed is  $\approx 0.6$ ; the others are reconstructed in one of the nearby pixels  
 $\implies$  some degradation of the spot size is introduced.
- If the average incidence angle of the photons is not perpendicular to the FS the MAPMT has to be shifted with respect to the lens.
- Prototypes have been built (quartz and Sol-Gel moulded lenses). Tests have been performed, others are in progress.
- A  $3 \times 3$  array coupled to MAPMTs has been tested:  
*Performance of a cluster of Multi-Anode Photomultipliers equipped with lenses for use in a prototype RICH detector*, CERN-EP/2001-051, 9 July, 2001, submitted to NIM A.
- Work plan:
  - optimize the design, given the incident light distribution;
  - find the best material;
  - evaluate the impact on the photo-detector.



## Performance of a cluster of Multi-anode Photomultipliers equipped with lenses for use in a prototype RICH detector

E. Albrecht<sup>1</sup>, J. Baker<sup>2</sup>, G. Barber<sup>3</sup>, J. Bibby<sup>4</sup>, M. Calvi<sup>5</sup>, M. Charles<sup>4</sup>, A. Duane<sup>3</sup>, S. Easo<sup>6a</sup>, S. Eisenhardt<sup>7</sup>, L. Eklund<sup>1</sup>, M. French<sup>2</sup>, V. Gibson<sup>8</sup>, A. Halley<sup>6</sup>, R. Halsall<sup>2</sup>, N. Harnew<sup>4</sup>, M.J.J. John<sup>3b</sup>, S.G. Katvars<sup>8</sup>, J. Libby<sup>4c</sup>, F. Muheim<sup>7</sup>, M. Paganoni<sup>5</sup>, A. Petrolini<sup>9</sup>, S. Playfer<sup>7</sup>, D. Price<sup>3</sup>, J. Rademacker<sup>4</sup>, N. Smale<sup>4</sup>, S. Topp-Jorgenson<sup>4</sup>, D. Websdale<sup>3</sup>, G. Wilkinson<sup>4</sup>, S.A. Wooton<sup>8</sup>

<sup>1</sup>CERN, European Organisation for Particle Physics, CH-1211 Geneva 23, Switzerland

<sup>2</sup>Rutherford Appleton Laboratory, Chilton, Didcot OX11 0QX, UK

<sup>3</sup>Imperial College of Science, Technology & Medicine, Blackett Laboratory, Prince Consort Road, London SW7 2AZ, UK

<sup>4</sup>Department of Physics, University of Oxford, Keble Road, Oxford OX1 3RH, UK

<sup>5</sup>Dipartimento di Fisica, Univ. di Milano-Bicocca and INFN-MILANO, Piazza della Scienza 3, 20126, Milan, Italy

<sup>6</sup>University of Glasgow, Department of Physics, Glasgow G12 8QQ, UK

<sup>7</sup>Department of Physics and Astronomy, University of Edinburgh, JCMB King's Buildings, Mayfield Road, Edinburgh EH9 3JZ, UK

<sup>8</sup>University of Cambridge, Cavendish Laboratory, Madingley Road, Cambridge CB3 0HE, UK

<sup>9</sup>Dipartimento di Fisica, Università di Genova and INFN, Via Dodecaneso 33, 16146, Genova, Italy

<sup>a</sup>Now at the Rutherford Appleton Laboratory

<sup>b</sup>Now at Collège de France, Lab. de Physique Corpusculaire, IN2P3-CNRS, 75231 Paris Cedex 05, France

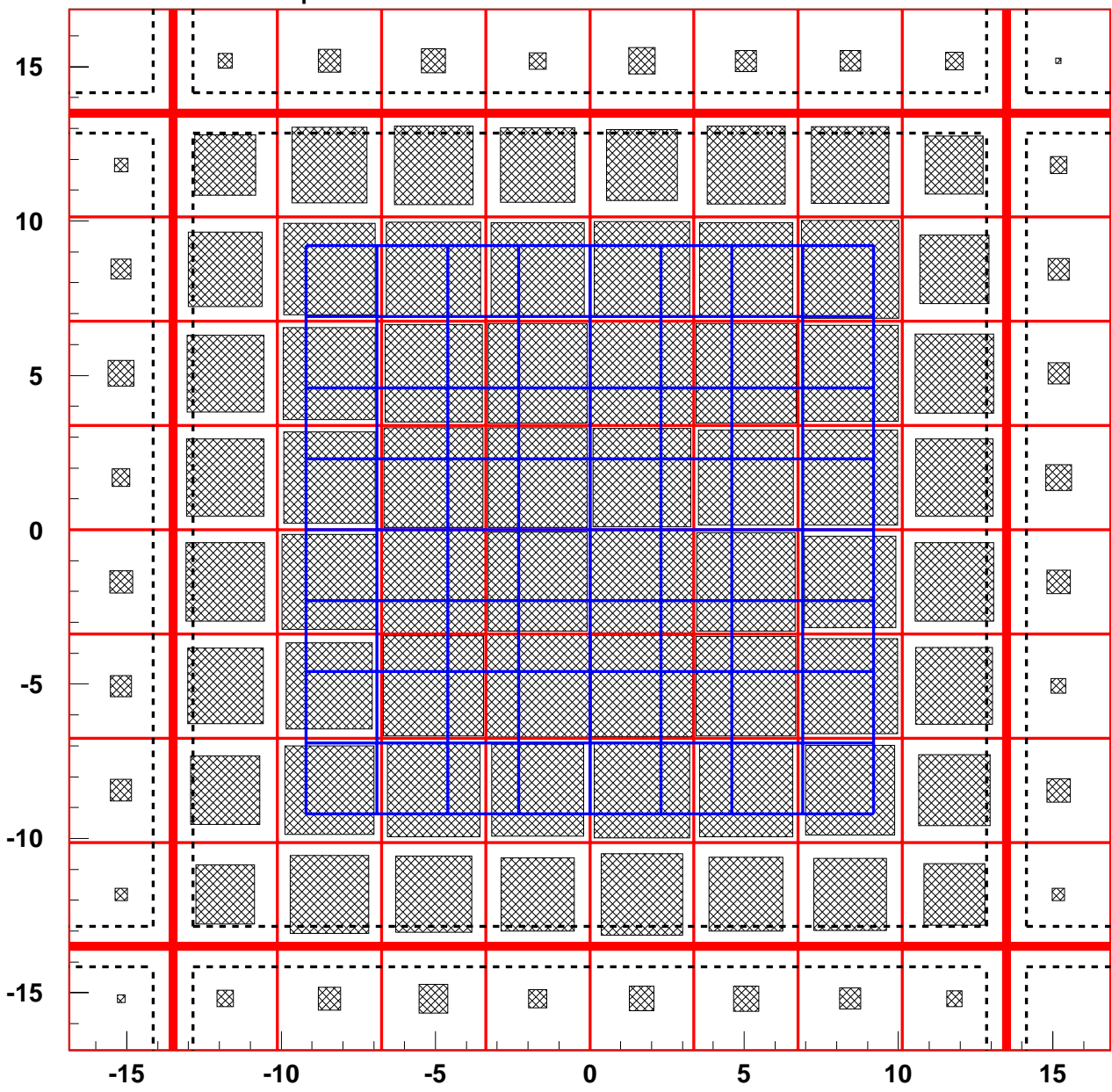
<sup>c</sup>Now at CERN

### Abstract

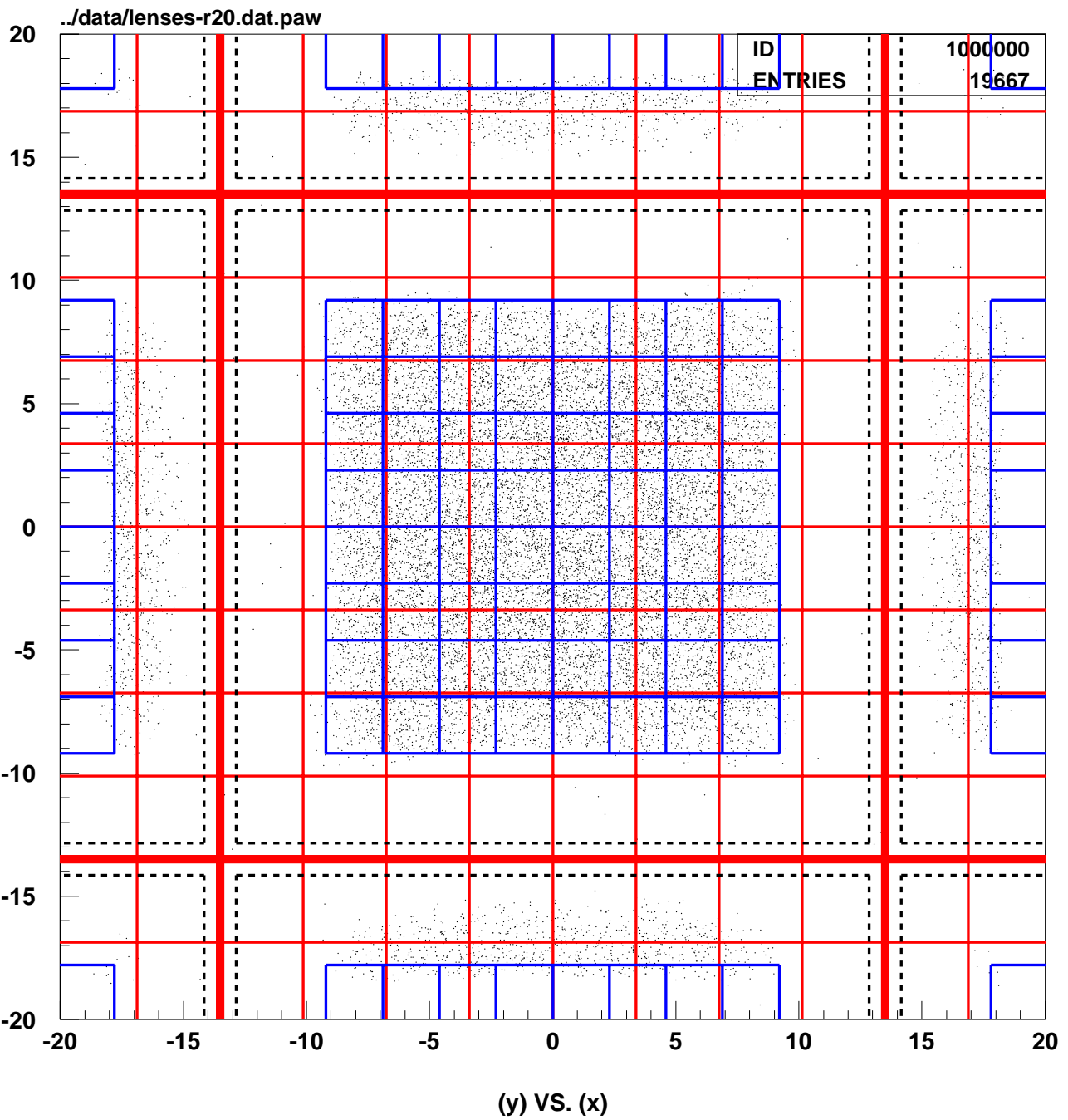
A cluster of Multi-anode Photomultiplier Tubes (MaPMTs) equipped with focusing lenses in front of the tubes was tested in a prototype Ring Imaging Čerenkov detector in a charged particle beam. The readout electronics were capable of capturing the data at 40 MHz. The effects due to charged particles and magnetic field on the MaPMT performance were also studied. The results are used to evaluate the MaPMT as a possible photodetector for the LHCb RICH detectors.

Submitted to Nucl. Instr. and Meth. A.

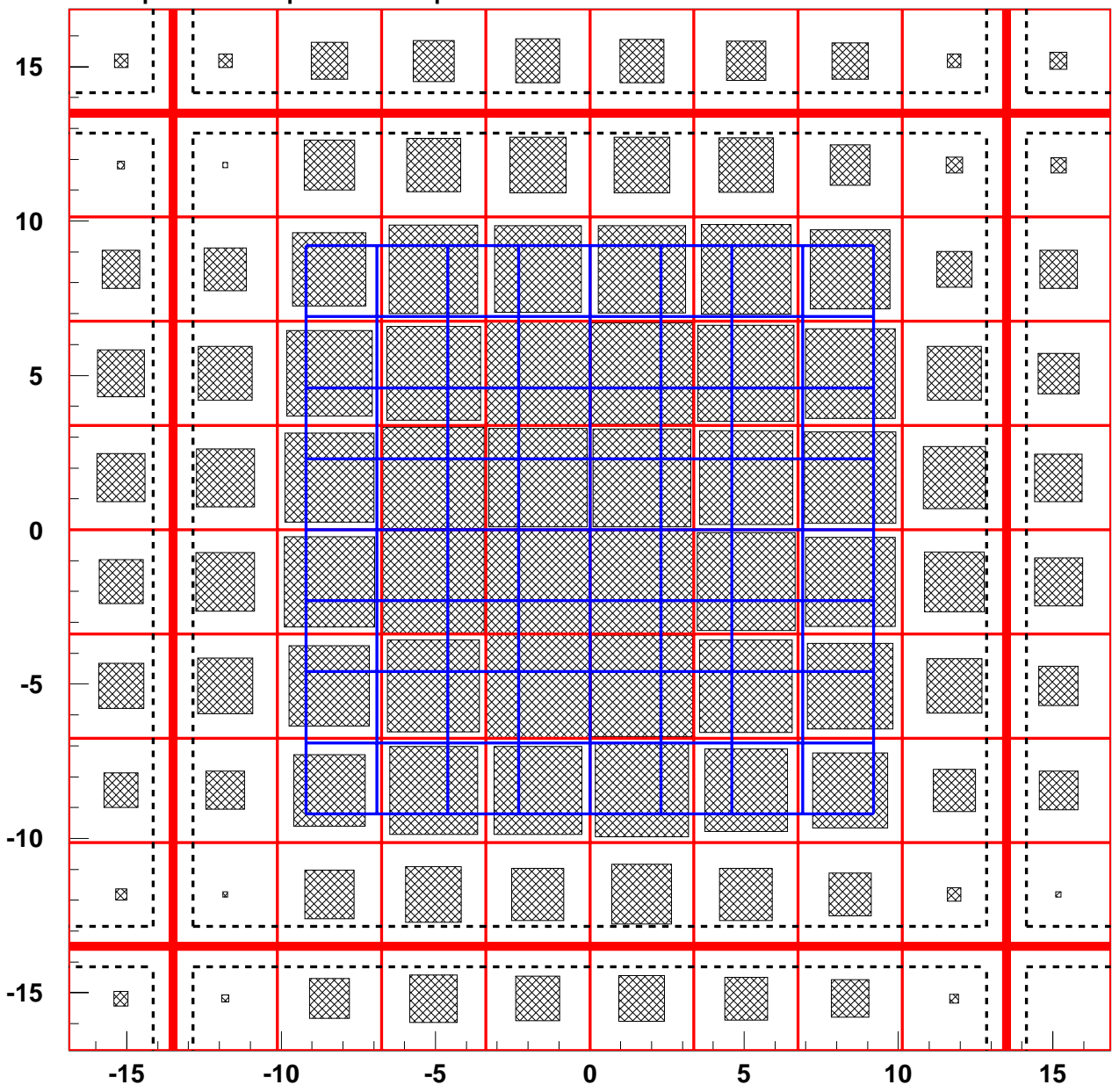
../data/lenses-r20.dat.paw



Reconstructed pixel (approximate binning)



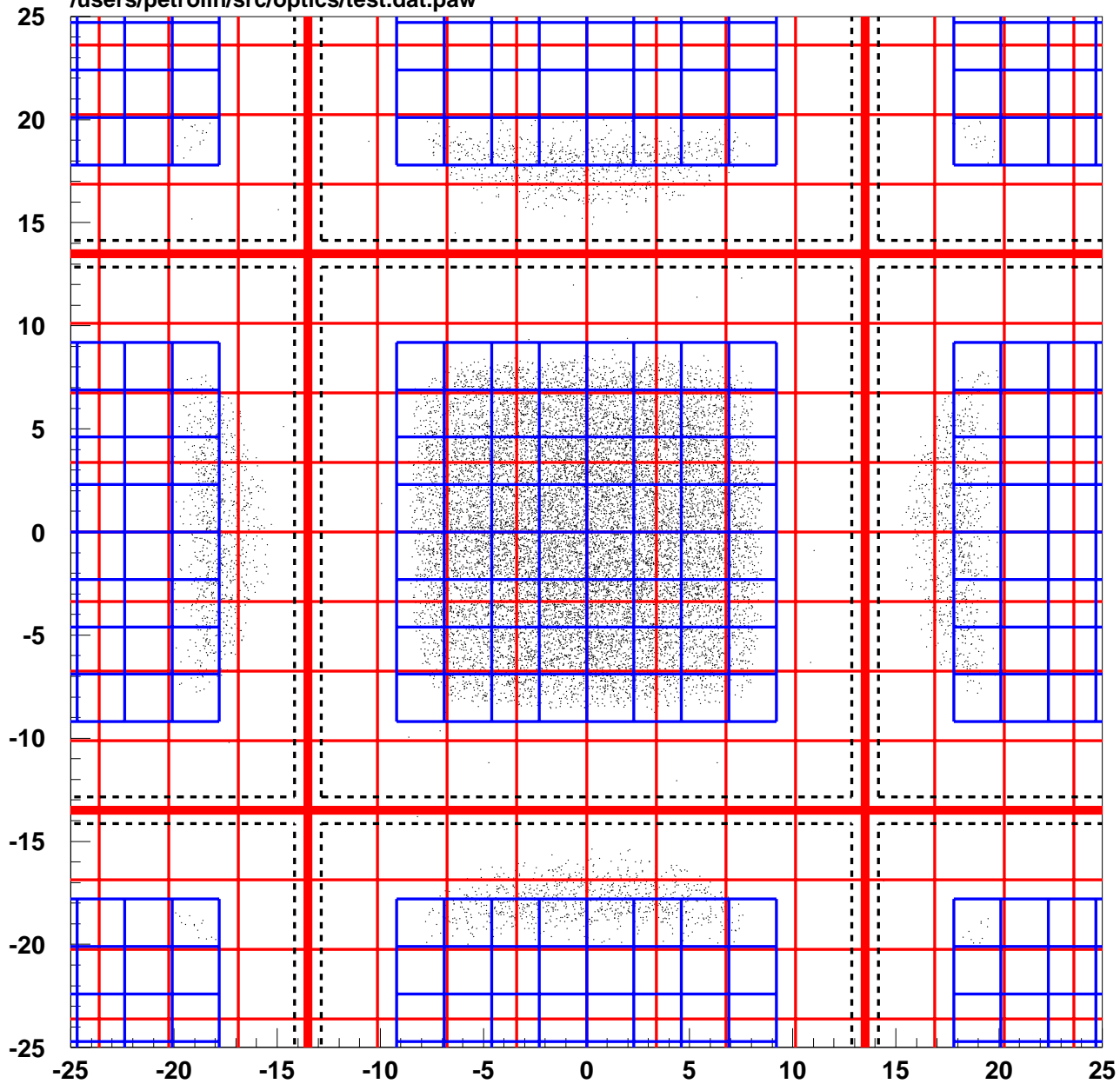
/users/petrolin/src/optics/test.dat.paw



Reconstructed pixel (approximate binning)



/users/petrolin/src/optics/test.dat.paw



(y) VS. (x)

# Lenses array performance

## New lens design

- Try to reduce the lens volume:  
this will reduce mass and bulk absorption
- New design with biconvex lens (promising).
- It needs to be optimized.

## Performance

Legenda:

RECO := fraction of reconstructed (i.e. detected) rays;

CREC := fraction of the RECO, reconstructed in the right pixel;

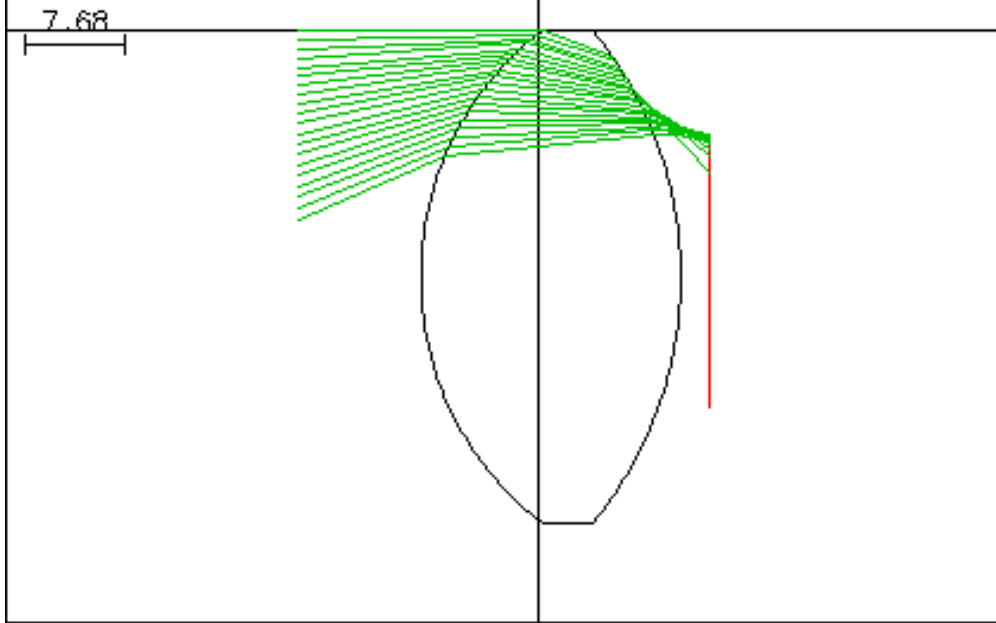
AINT := average intensity of the reconstructed rays;

GEFF := overall detection efficiency.

	RECO	CREC	AINT	GEFF
r20t15	0.89	0.88	0.89	0.70
r20t20	0.86	0.85	0.89	0.68
r20t25	0.84	0.82	0.89	0.66
r24t15	0.85	0.88	0.89	0.68
r24t20	0.82	0.85	0.89	0.65
r24t25	0.77	0.82	0.89	0.61
BBBt15	0.91	0.53	0.88	0.72
BBBt20	0.89	0.51	0.88	0.70
BBBt25	0.85	0.49	0.88	0.66

No name  
OPTICAL SYSTEM LAYOUT

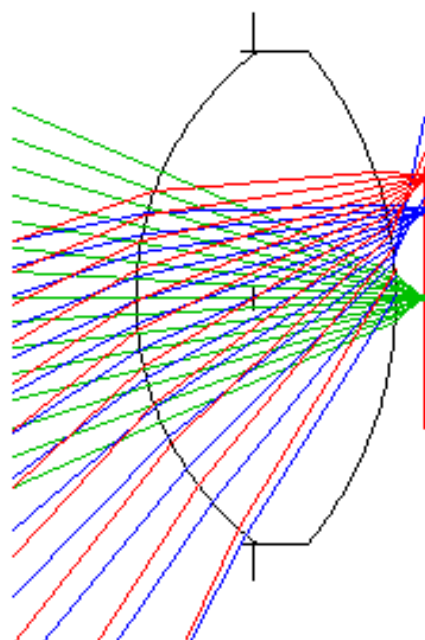
UNITS: MM  
DES: OSLO



No name  
OPTICAL SYSTEM LAYOUT

UNITS: MM  
DES: OSLO

7.68



FULL FIELD  
0.37deg



0.7 FIELD  
0.259deg



ON-AXIS  
0deg

♀



-0.01

-0.005

0

0.005

0.01

FOCUS SHIFT

SPOT SIZE & FOCUS SHIFT: UNITS =  $\mu\text{m}$   
WAVELENGTHS ( $\mu\text{m}$ )  
W1: 0.38 W2: 0.4 W3: 0.3

No name  
SPOT DIAGRAM ANALYSIS

OSLO  
30 sep 01  
05:02 PM

# Information for the photo-detector design

A lot of information is urgently needed (right now !)  
for the photo-detector design and simulation.

## Atmospheric physics

- Photon transport into the atmosphere:  
probability that a photon produced at  $\mathbf{x}$  will reach  $\mathbf{y}$ ,  
as a function of  $(\mathbf{x}, \mathbf{y})$ .

## Main optics

- Geometrical shape and dimensions of the focal surface.
- Parameterization of the mapping of the light impinging  
on the optics at an angle  $\theta$  with the axis  
to the centroid of its spot on the FS:  $\theta \rightarrow (u, v)$   
 $[(\theta, \phi, x, y) \rightarrow (u, v, T)]$
- Overall light transmission and PSF  
as a function of the angle from the axis.
- Distribution of the incidence angle of the photons  
on the focal surface as a function of the angle from the axis.
- The PSF should be, possibly, optimized at the angle  $\bar{\theta} \gg 0$   
such that the average PSF on the focal surface,

$$\langle \text{PSF} \rangle \propto \int \int \text{PSF}(\theta) \sin \theta d\theta d\phi$$

is maximized

# Detailed experimental apparatus simulation

- Single photon overall detection efficiency.
- EAS image (taking into account a realistic FS design).
- EAS reconstruction.
- Simulation of all the background sources to estimate:
  - required power consumption and ageing of the MAPMTs;
  - dead/recovery times;
  - noise induced by cosmic rays on EUSO;
  - stray light on the FS produced by strong light sources.

# Conclusions

## Micro-cell design

- A functional design has been carried on, tests are in progress.
- Space qualification issues are being studied.
- Aim to produce a new version, with improvements, during phase A.

## FS layout and macro-cell design

- A realistic arrangement of the FS layout and a tentative design of the supporting structure were proposed.
- A preliminary design of the macrocell structure was done, compatible with micro-cell and FS layout.
- Aim to produce a realistic preliminary functional design, during phase A.

## Optical adapters

- The performance of different systems was carefully simulated in realistic conditions.
- Further optimization is required.